NIH Public Access
Author Manuscript
Opt Lett. Author manuscript; available in PMC 2010 August 13.

Published in final edited form as:
Opt Lett. 2010 February 1; 35(3): 426–428.

High speed line-scan confocal imaging of stimulus-evoked intrinsic optical signals in the retina

Yang-Guo Li[1], **Lei Liu**[2], **Franklin Amthor**[3], and **Xin-Cheng Yao**[1,*]

[1]Department of Biomedical Engineering, University of Alabama at Birmingham, Birmingham, AL 35294

[2]Department of Optometry, University of Alabama at Birmingham, Birmingham, AL 35294

[3]Department of Psychology, University of Alabama at Birmingham, Birmingham, AL 35294

Abstract

A rapid line-scan confocal imager was developed for functional imaging of the retina. In this imager, an acousto-optic deflector (AOD) was employed to produce mechanical vibration- and inertia-free light scanning, and a high-speed (68,000 Hz) linear CCD camera was used to achieve sub-cellular and sub-millisecond spatiotemporal resolution imaging. Two imaging modalities, i.e., frame-by-frame and line-by-line recording, were validated for reflected light detection of intrinsic optical signals (IOSs) in visible light stimulus activated frog retinas. Experimental results indicated that fast IOSs were tightly correlated with retinal stimuli, and could track visible light flicker stimulus frequency up to at least 2 Hz.

Intrinsic optical signals (IOSs) have been detected in retinal photoreceptors (1) and other neural tissues (2). The IOSs usually consist of both stimulus-evoked retinal neural activity and corresponding hemodynamic and metabolic changes. While IOSs associated with hemodynamic and metabolic changes (3,4) can provide important information about the physiological well-being of the retina, they are relatively slow and thus cannot be used to assess fast retinal neural activities. It has been shown that fast IOSs have the time courses comparable to that of retinal electrophysiological kinetics (5,6). Imaging fast IOSs may provide a new method to evaluate the functional integrity of photoreceptors and inner neurons. Without complications of hemodynamic changes and eye movements, isolated retinas can provide a simple preparation for understanding the sources and biophysical mechanism of fast IOSs, and also for optimizing the design of retinal imaging instruments. A transmitted light microscope has been used to validate the feasibility of imaging fast IOSs in isolated amphibian (frog and salamander) retinas (6,7). Although transmitted light imaging can provide valuable information for advanced study of visual information processing in the retina, reflected light recording modality is typically required for potential *in vivo* application of fast IOSs. Optical recordings of stimulus-evoked transient IOSs in the eye have been successfully demonstrated (3,4,8–12), but reliable imaging of fast IOSs is still a challenge to researchers (10). Both time-domain (13,14) and frequency-domain (12) optical coherence tomography (OCT) imagers have been used for depth-resolved recording of IOSs in the retina. While the imaging speed of time-domain OCT is limited by time-consuming scanning requirement of the light probe; transversal resolution of frequency-domain OCT is compromised because of unavoidable blur of out-of-focus light (15). Line-scan imaging (15–17) may provide a practical strategy for high spatiotemporal resolution

*Corresponding author: xcy@uab.edu.

OCIS codes: 170.2655 Functional monitoring and imaging; 330.5310 Vision - photoreceptors.

NIH-PA Author Manuscript
NIH-PA Author Manuscript
NIH-PA Author Manuscript

NIH-PA Author Manuscript

NIH-PA Author Manuscript

NIH-PA Author Manuscript

imaging. Here, we report a rapid line-scan confocal imager to achieve reflected light imaging of stimulus-evoked fast IOSs in frog retinas.

Figure 1a illustrates the schematic diagram of our rapid line-scan confocal imager. While a visible light (~10^5 550-nm photons·μm^{-2}· ms^{-1}) was used for retinal stimulation, a near infrared (NIR) light (central wavelength: 790 nm; spectral bandwidth: ~2nm) was used for imaging fast IOSs. In order to achieve a line-focus illumination at the sample plane, a cylindrical lens was used to condense the NIR light in one dimension. An acousto-optic deflector (AOD) (LS55-NIR, ISOMET) was used to achieve rapid, mechanical vibration- and inertia-free scanning of the NIR light. A fast linear CCD camera (SG-11-01k80-00R, DALSA) with pixel size of 14um×14um was employed to achieve imaging speed up to 68,000 lines per second. With a 10×/0.25 objective, this confocal system can achieve a transversal resolution of < 2.0μm. At this sub-cellular transversal resolution, individual photoreceptors can be clearly identified, as shown in Fig. 1b. Using a piezo nanofocusing system (P-720, Physik Instrumente) to change the focus of the objective, axial resolution (Fig. 1c) of this system was tested by placing a mirror at the sample plane. From Fig. 1c, we can see that the axial resolution of this imager is ~ 12μm, which is smaller than the length of the photoreceptors (18). In other words, this rapid confocal imager can image fast IOSs from the photoreceptor with sub-cellular spatial resolution in both transversal and axial directions.

Isolated frog (*Rana Pipiens*) retinas were used to validate reflected light confocal imaging of fast IOSs in stimulus activated photoreceptors. The experiment procedures were approved by the Institutional Animal Care and Use Committee of University of Alabama at Birmingham. The experiment was conducted in a dark environment with dim red light illumination. Frogs were dark-adapted for 20–30min at first. Then rapid euthanasia and retina isolating surgery were conducted. The isolated retina was transferred to a recording chamber which was filled with Ringer's solution. During the recording, the retina was continuously illuminated by a ~300μW NIR light, and the confocal imager was focused at the photoreceptor layer of the retina. Two imaging modalities, i.e., frame-by-frame and line-by-line recording, were validated for reflected light imaging of fast IOSs. The frame-by-frame and line-by-line modalities could be readily switched by controlling synchronization signals of the AOD scanner and CCD imager.

Figure 2 shows frame-by-frame confocal imaging of reflected light IOSs in frog retinas. For the experiment shown in Fig.2, a 0.5s pre-stimulus baseline was recorded before a visible white light stimulus flash was delivered to the retina, and a 2.5 s post-stimulus image sequence was recorded. Both positive (i.e., increasing) and negative (i.e., decreasing) optical changes were observed in the IOS images (Fig. 2c). At sub-cellular level, the peak magnitude of localized IOSs (traces 1–6 in Fig. 2d) could be as high as 30% ΔI/I (traces 1–6 in Fig. 2d), where ΔI was dynamic optical change and I was pre-stimulus baseline intensity. However, the overall IOS (trace 7 in Fig. 2d) averaged over the entire image area was one order of magnitude smaller due to the integral effect of the IOSs with opposite (i.e., positive and negative) polarities. As shown in Fig. 2d, fast IOSs, at least the early phase of the IOSs, have comparable time courses with the ERG response. The onset phase of fast IOSs occurred immediately after the stimulus onset, but the recovery phase of IOSs was relatively slow (Fig. 2d). The statistics of activated retinal areas with positive and negative IOSs further supported the existence of both fast (black arrow in Fig. 2e) and slow IOSs (grey arrow in Fig. 2e). We hypothesize that the fast IOSs were directly related to early phototransduction procedures in the photoreceptors; while the slow IOSs were resulted from later phototransduction procedures and metabolic dynamics of the retina.

When the system was configured in the line-by-line recording mode, the temporal resolution of the system could go up to 14.7μs (i.e., 68,000 Hz). During line-by-line recording, the

NIH-PA Author Manuscript

NIH-PA Author Manuscript

NIH-PA Author Manuscript

driver of the AOD scanner was sustained at a fixed voltage, and thus the NIR light probe would be fixed at a line area of the retina. Line-by-line imaging (e.g., M-sequence image) can provide simultaneous depiction of temporal (lateral coordination) and spatial (vertical coordination) dynamics of the IOSs, and is suitable for investigating IOS dynamics at an ultra-high temporal resolution. Figure 3 represents line-by-line recording of reflected light IOSs in frog retinas. During the experiment, the system was first set in frame-by-frame mode for easy identification of location of interest for line-by-line recording. Unlike a single flash stimulus for the experiment shown in Fig. 2, a 2Hz visible light flicker was employed for line-by-line recording. The duration of the 2Hz flicker stimulus was 2.0 s (i.e., 4 pulses). A 0.5s pre-stimulus and 4.5 s post-stimulus image sequence was recorded for evaluation of the IOSs evoked by the flicker stimuli. In addition to the IOS images shown in Fig. 3b, Fig. 3c shows dynamic differential IOS (DIOS) images in order to achieve better visualization of the frequency correlation of the IOSs and flicker stimuli. The DIOS image was constructed by subtracting the average of previous 10 ms recordings from the current measurement sequentially. Fig. 3e shows dynamic DIOSs at the selected sites. The dynamic differential processing acted as a high-pass filter to separate fast IOSs changes from slow IOSs in the photoreceptor. Flicker stimuli consistently disclosed stepped increases of the IOSs, with peak magnitude as high as 40% $\Delta I/I$ (trace 3 in Fig. 3d). This observation supports our hypothesis that rapid IOSs recorded from the photoreceptor layer might be directly correlated with early phototransduction procedures, and the IOS peak magnitude saturation (e.g., trace 3 in Fig. 3d) might be correlated with the pigment bleaching level (19) due to the repeated flicker stimuli. The statistics of activated retinal areas with positive and negative optical responses disclosed that fast IOSs occurred within 5 ms after the stimulus onset (Fig. 3e), which is consistent with previous transmitted light investigation of fast IOSs (6,20).

In summary, a high speed line-scan confocal system was developed for reflected light imaging of fast IOSs correlated with stimulus-evoked retinal activation. Two imaging modalities, i.e., frame-by-frame and line-by-line recording, were validated for reflected light imaging of IOSs in frog retinas. Because of the effective rejection of out-of-focus background light, fast confocal imaging typically produced fast IOSs with magnitude peak up to 40% $\Delta I/I$ (trace 3 in Fig. 3d). Our experimental results indicated that fast IOSs were tightly correlated with retinal responses to light stimuli, and could track at least 2 Hz visible light flicker. We hypothesize that fast IOSs at stimulus activated photoreceptors may be directly correlated with early phototransduction procedures. Our experiments suggest that dynamic DIOS processing may provide a simple, but effective way, to separate fast IOSs from slow IOSs in the retina. In coordination with sophisticated retinal stimulation and data processing, we anticipate that further improvements, such as integration of adaptive optics to compensate for ocular aberrations and combination of OCT to improve axial resolution, of the line-scan confocal imager, may pave the way toward practical applications of fast IOSs imaging in high resolution study and diagnosis of retinal function.

Acknowledgments

This research was supported by NIH (1R21RR025788-01), Eyesight Foundation of Alabama, and DANA Foundation (Brain and Immuno-Imaging Grant Program).

References

1. Pepperberg DR, Kahlert M, Krause A, Hofmann KP. Photic modulation of a highly sensitive, near-infrared light-scattering signal recorded from intact retinal photoreceptors. Proc Natl Acad Sci U S A 1988;85(15):5531–5535. [PubMed: 3399504]

2. Cohen LB, Keynes RD, Hille B. Light scattering and birefringence changes during nerve activity. Nature 1968;218(5140):438–441. [PubMed: 5649693]

NIH-PA Author Manuscript

NIH-PA Author Manuscript

NIH-PA Author Manuscript

3. Nelson DA, Krupsky S, Pollack A, Aloni E, Belkin M, Vanzetta I, Rosner M, Grinvald A. Special report: Noninvasive multi-parameter functional optical imaging of the eye. Ophthalmic Surg Lasers Imaging 2005;36(1):57–66. [PubMed: 15688972]
4. Abramoff MD, Kwon YH, Ts'o D, Soliz P, Zimmerman B, Pokorny J, Kardon R. Visual stimulus-induced changes in human near-infrared fundus reflectance. Invest Ophthalmol Vis Sci 2006;47(2): 715–721. [PubMed: 16431972]
5. Schei JL, McCluskey MD, Foust AJ, Yao XC, Rector DM. Action potential propagation imaged with high temporal resolution near-infrared video microscopy and polarized light. Neuroimage 2008;40(3):1034–1043. [PubMed: 18272402]
6. Yao XC, Zhao YB. Optical dissection of stimulus-evoked retinal activation. Opt Express 2008;16(17):12446–12459. [PubMed: 18711481]
7. Zhao YB, Yao XC. Intrinsic optical imaging of stimulus-modulated physiological responses in amphibian retina. Opt Lett 2008;33(4):342–344. [PubMed: 18278104]
8. Srinivasan VJ, Wojtkowski M, Fujimoto JG, Duker JS. In vivo measurement of retinal physiology with high-speed ultrahigh-resolution optical coherence tomography. Opt Lett 2006;31(15):2308–2310. [PubMed: 16832468]
9. Jonnal RS, Rha J, Zhang Y, Cense B, Gao W, Miller DT. In vivo functional imaging of human cone photoreceptors. Opt Express 2007;15(24):16141–16160.
10. Grieve K, Roorda A. Intrinsic signals from human cone photoreceptors. Invest Ophthalmol Vis Sci 2008;49(2):713–719. [PubMed: 18235019]
11. Hanazono G, Tsunoda K, Kazato Y, Tsubota K, Tanifuji M. Evaluating neural activity of retinal ganglion cells by flash-evoked intrinsic signal imaging in macaque retina. Invest Ophthalmol Vis Sci 2008;49(10):4655–4663. [PubMed: 18539934]
12. Srinivasan VJ, Chen Y, Duker JS, Fujimoto JG. In vivo functional imaging of intrinsic scattering changes in the human retina with high-speed ultrahigh resolution OCT. Opt Express 2009;17(5): 3861–3877. [PubMed: 19259228]
13. Yao XC, Yamauchi A, Perry B, George JS. Rapid optical coherence tomography and recording functional scattering changes from activated frog retina. Appl Opt 2005;44(11):2019–2023. [PubMed: 15835350]
14. Bizheva K, Pflug R, Hermann B, Povazay B, Sattmann H, Qiu P, Anger E, Reitsamer H, Popov S, Taylor JR, Unterhuber A, Ahnelt P, Drexler W. Optophysiology: depth-resolved probing of retinal physiology with functional ultrahigh-resolution optical coherence tomography. Proc Natl Acad Sci U S A 2006;103(13):5066–5071. [PubMed: 16551749]
15. Chen Y, Huang SW, Aguirre AD, Fujimoto JG. High-resolution line-scanning optical coherence microscopy. Opt Lett 2007;32(14):1971–1973. [PubMed: 17632613]
16. Hammer DX, Ferguson RD, Ustun TE, Bigelow CE, Iftimia NV, Webb RH. Line-scanning laser ophthalmoscope. J Biomed Opt 2006;11(4) 041126.
17. Im KB, Han S, Park H, Kim D, Kim BM. Simple high-speed confocal line-scanning microscope. Opt Express 2005;13(13):5151–5156. [PubMed: 19498504]
18. Hoang QV, Linsenmeier RA, Chung CK, Curcio CA. Photoreceptor inner segments in monkey and human retina: mitochondrial density, optics, and regional variation. Vis Neurosci 2002;19(4):395–407. [PubMed: 12511073]
19. Kahlert M, Pepperberg DR, Hofmann KP. Effect of bleached rhodopsin on signal amplification in rod visual receptors. Nature 1990;345(6275):537–539. [PubMed: 2161501]
20. Yao XC. Intrinsic optical signal imaging of retinal activation. Jpn J Ophthalmol 2009;53(4):327–333. [PubMed: 19763749]

NIH-PA Author Manuscript
NIH-PA Author Manuscript
NIH-PA Author Manuscript

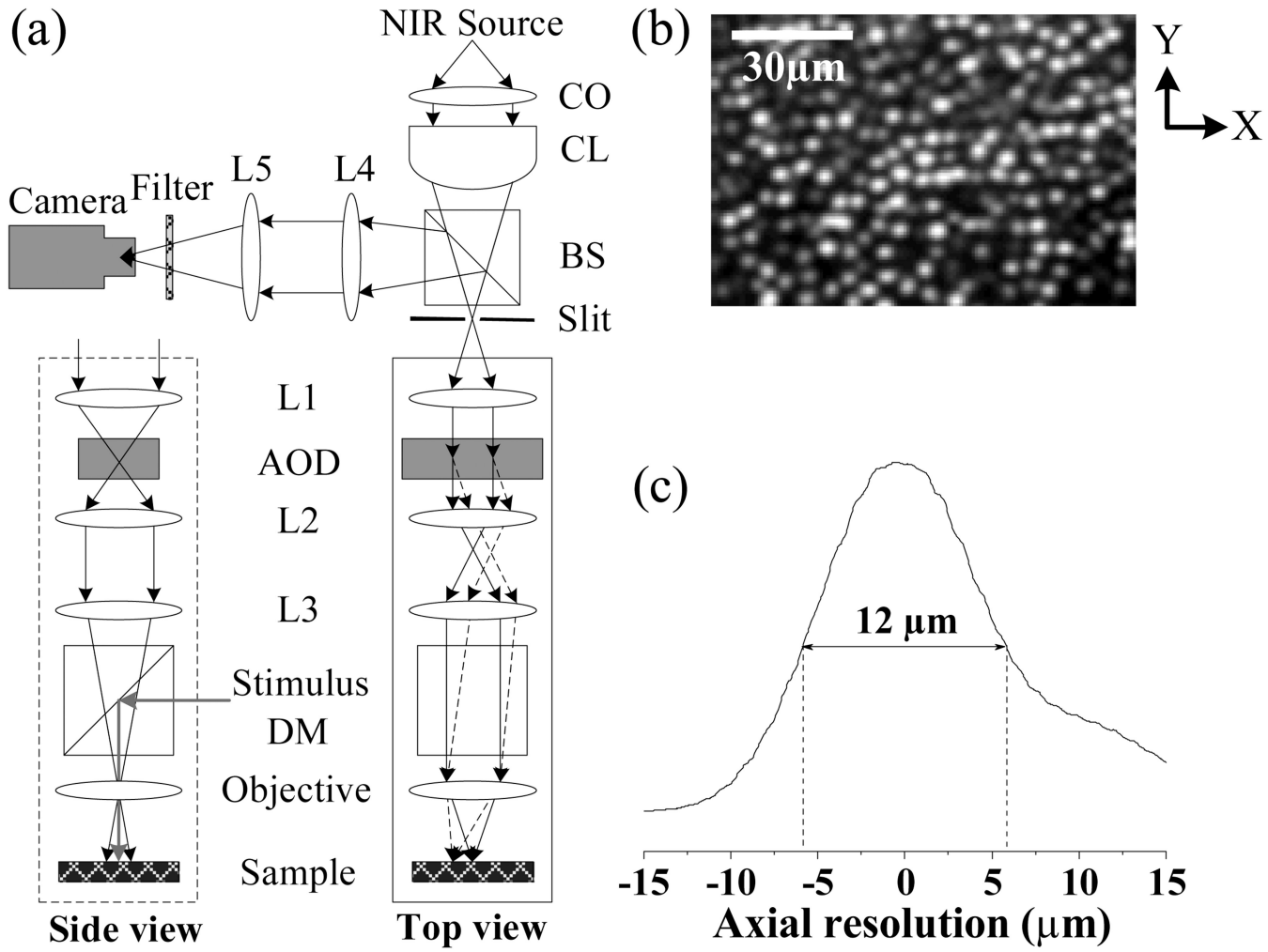

Fig. 1.

(a) Schematic diagram of line-scan confocal system. CO: collimator; CL: cylindrical lens BS: beam splitter; AOD: acousto-optic deflector; DM: dichroic mirror; Lx: spherical lenses. Focal length of the CL is 50 mm. Focal length of the lenses L1–L5 are 80mm, 60mm, 120mm, 60mm, and 100mm, respectively. (b) Confocal image showing clear cellular structure of individual photoreceptors. In the x direction (i.e., parallel to the focused scanning line), theoretical resolution of the imager is ~ 1.9 μm (0.61λ/NA). In the y direction (i.e., perpendicular to the focused scanning line), theoretical resolution of the imager is ~ 1.3 μm (0.4λ/NA). (c) Axial resolution of line-scan confocal imaging system was tested to be ~ 12 μm.

NIH-PA Author Manuscript

NIH-PA Author Manuscript

NIH-PA Author Manuscript

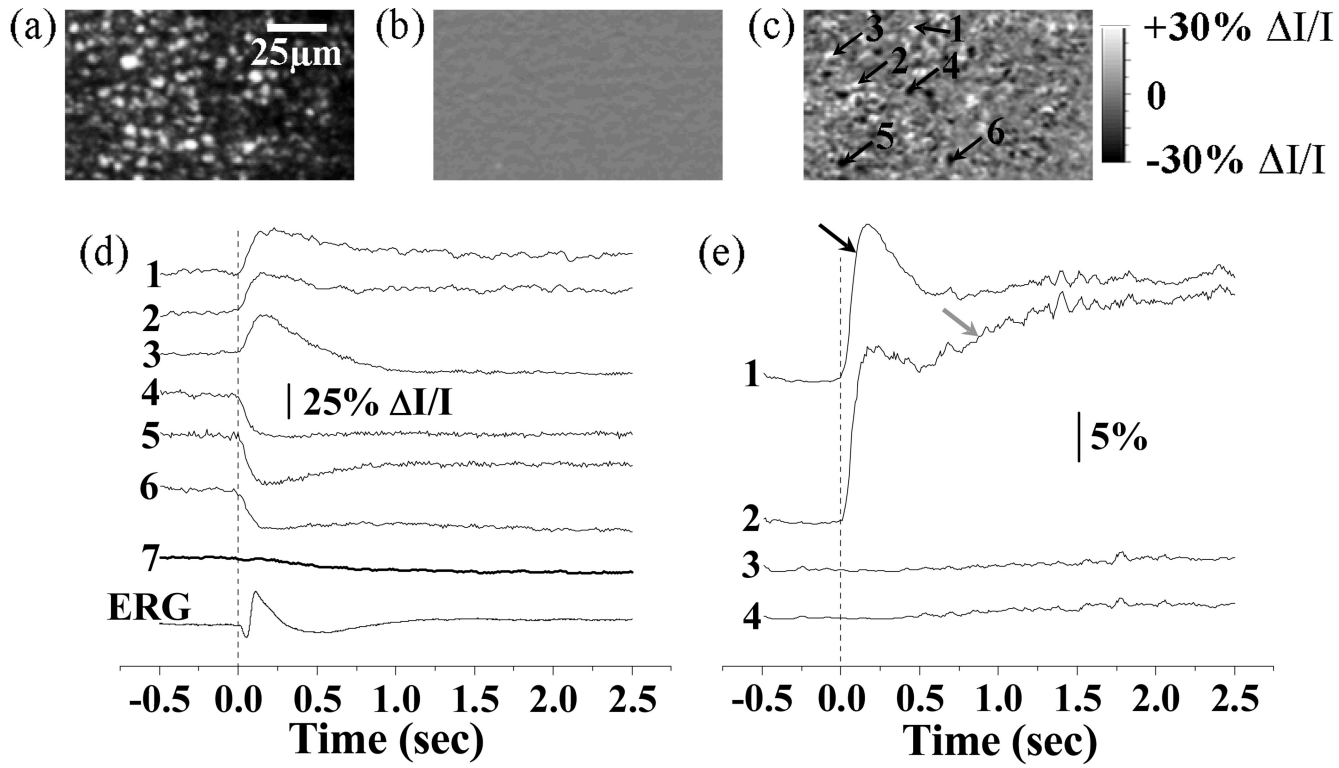

Fig. 2.

Frame-by-frame imaging of IOSs. (a) Raw image of photoreceptors. (b) Pre-stimulus IOS image. (c) Post-stimulus IOSs image. The raw confocal images were acquired at the speed of 100 frames/s, with NIR imaging light focused at photoreceptor layer. Both pre-stimulus and post-stimulus IOSs images were an average over 250 ms. (d) Tracings 1–6 revealed the IOSs variation property of local areas pointed by arrowheads 1–6 in (c). Tracing 7 represents integral IOSs by averaging all the pixels of each IOS image. Vertical line indicates the onset of the stimulus. (e) The percentage statistics of activated retinal areas with positive (> 5% ΔI/I) and negative (< −5% ΔI/I) IOSs. The threshold (5%ΔI/I) was used to reduce the effect of background noise on the statistics. Trace 1 (positive IOSs) and 2 (negative IOSs) are statistic results of experiment trial with stimulus delivered. Trace 3 (positive IOSs) and 4 (negative IOSs) are statistic results of control trial without stimulus.

NIH-PA Author Manuscript

NIH-PA Author Manuscript

NIH-PA Author Manuscript

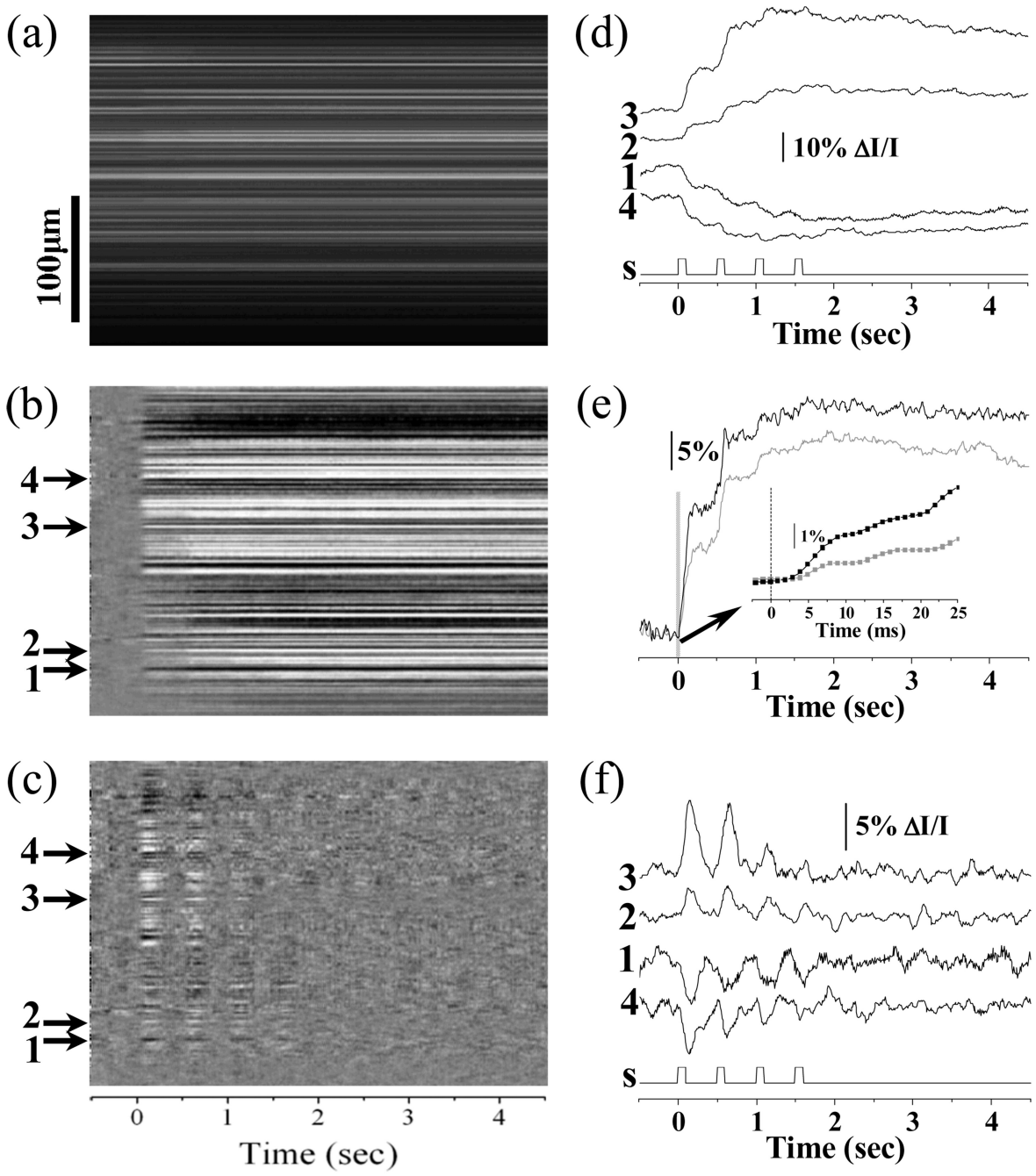

Fig. 3.

Line-by-line imaging of IOSs. (a) Line-by-line raw image; (b) Line-by-line IOS image; (c) Line-by-line DIOS image. (d) Representative localized IOSs (arrows 1–4). S: visible light stimulus. (e) The statistics of activated retinal area ratios with positive (black) and negative (grey) IOSs. Inset panel shows enlarged picture of early optical response marked by the gray bar. Rapid IOSs occurred within 5ms after stimulus onset (inset panel). (f) Representative localized DIOSs (arrows 1–4).